Realization of quantum efficiency enhanced PIN photodetector by assembling resonant waveguide grating

Jinhua Hu (胡劲华), Yongqing Huang (黄永清)*, Xiaomin Ren (任晓敏), Xiaofeng Duan (段晓峰), Yehong Li (李业弘), and Yang Luo (骆 扬)

State Key Laboratory of Information Photonics and Optical Communications, Institute of Information Photonics and Optical Communications, Beijing University of Posts and Telecommunications, Beijing 100876, China

Corresponding author: yqhuang@bupt.edu.cn

Received February 26, 2014; accepted April 4, 2014; posted online June 20, 2014

We demonstrate an InP/InGaAs PIN photodetector with enhanced quantum efficiency by assembling silicon resonant waveguide gratings for the application of polarization sensitive systems. The measured results show that quantum efficiency of the photodetector with silicon resonant waveguide gratings can be increased by 31.6% compared with that without silicon resonant waveguide gratings at the wavelength range of 1500 to 1600 nm for TE-polarization.

OCIS codes: 230.5160, 230.5440, 050.2770.

doi: 10.3788/COL201412.072301.

High-efficiency photodetector is attractive for its potential applications in polarization sensitive systems[1−3]. For a conventional PIN photodetctor, the thickness of absorption layer is a critical parameter, which can influence absorption and carrier transition time. With increasing the thickness, the optical absorption was enhanced and simultaneously the carrier transition time prolonged. Therefore, there is a tradeoff between the quantum efficiency and the operating bandwidth since the operating bandwidth will decrease with increase of the quantum efficiency[4]. To improve the quantum efficiency of PIN photodetetor in polarization sensitive systems, high-reflectivity (HR) mirrors with polarization selectivity can be utilized while maintaining the bandwidth. Recently, HR mirrors have been reported to improve the quantum efficiency of PIN photodetectors. However, the most common HR mirror[5] is mainly based on distributed Bragg reflector (DBR) which has the reflectivity of more than 99% and usually requires a multitude of layers with each having precise control of layer thicknesses and refractive index. On the other hand, Yuan *et al.*[6] used a Ti/Au-SiO_2 phase-matcher layer as HR mirror to improve the quantum efficiency of InGaAs /InP photodetector at the wavelength of 1550 nm. Duan *et al.*[7] proposed a SOI-Based concentric circular subwavelength grating as HR mirror to enhance the quantum efficiency of InGaAs/InP PIN photodetetor. However, the above mentioned HR mirrors, which are polarization insensitive, are not suitable for the application of polarization sensitive systems. In recent years, silicon guided-mode resonant (GMR) grating has emerged as an important functional device in photonic integrated circuits due to its high polarization sensitivity and reflection[8,9]. Silicon is an excellent material with lower absorption loss in optical communication wavelength ranging from 1400 to 1600 nm. Silicon GMR grating exhibits greater advantage in terms of loss, polarization sensitivity and reflection compared to metal grating and multi-layer stacks. Therefore silicon GMR is a better candidate as HR mirror for PIN photodetectors.

In this letter, we demonstrated a broadband, quantum-efficiency-enhanced photodetetor by using silicon polarization selective GMR grating structure as HR mirrors. The GMR grating structure had high reflection over 100-nm wavelength range for TE-polarization. A vertical-illuminated InGaAs/InP absorption structure was fabricated and its quantum efficiency was significantly enhanced by the GMR grating.

Schematic diagram of the vertical-illuminated photodetector structure is shown in Fig. 1, where an InGaAs/InP PIN absorption structure and a silicon GMR grating are assembled. The PIN absorption structure was designed according to Ref. [10]. The GMR grating is designed with 100-nm bandwidth using rigorous coupled-wave analysis (RCWA)[11,12] and model method[13]. The

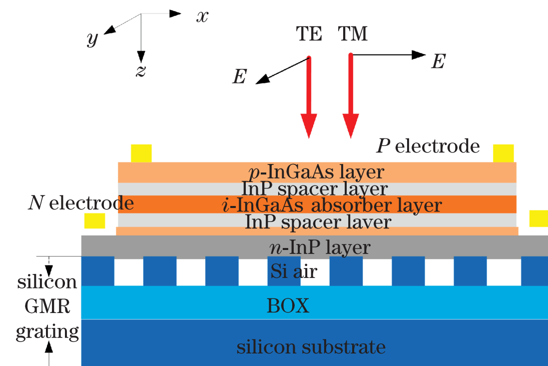

Fig. 1. (Color online) Schematic diagram of the proposed photodetector structure.

Table 1. Parameters of the InGaAs/InP Absorption Structure

Structure	Thickness (nm)	Index
InP n Contact Layer	162	3.17
InGaAs Etch Stop Layer	40	3.56
InP Spacer Layer	122	3.17
i-InGaAs Absorbing Layer	384	3.60-i0.0965
InP Spacer Layer	244	3.17
InGaAs p Contact Layer	200	3.56

 © 2014 Chinese Optics Letters

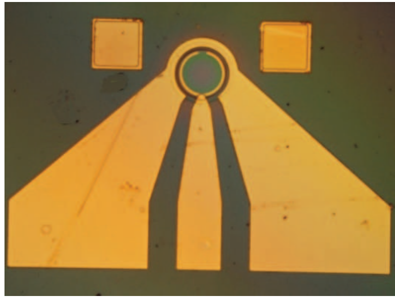

Fig. 2. (Color online) Top-view optical micrograph of the fabricated InGaAs/InP absorption structure.

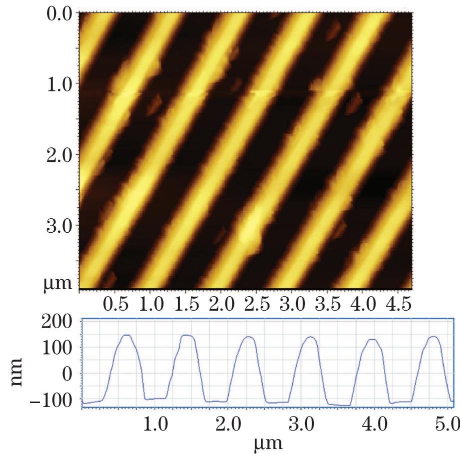

Fig. 3. (Color online) AFM image and profile of the fabricated silicon guided-mode resonance grating structure.

normal incident light is firstly coupled into the InGaAs p contact layer and then through the InP spacer layer, which is designed to decrease the dark current, partly absorbed by the i-InGaAs layer of the PIN structure, the light is finally reflected by the GMR grating, and again absorbed by the i-InGaAs layer. Here, TE polarization with E-field polarizing along y direction, and TM polarization along the x direction are taken into account.

The GMR grating structure was fabricated on a SOI wafer with 220-nm Si top layer and 3-μm buried oxide (BOX) layer. The grating structure was firstly patterned with a positive photo-resist ZEP520 by electron-beam lithography and then transferred into the top Si layer by inductively coupled plasma reactive ion etching (ICP-RIE). Parameters of the InP/InGaAs PIN absorption structure, which was fabricated by standard photolithography lithography and chemical selective wet etching is shown in Table 1. An absorption structure was grown by low-pressure metal organic-chemical vapor deposition (MOCVD) on a semi-insulating InP substrate, and followed a deposition of 120-nm InP cap layer. Fabrication of the photodetector was as follows. Firstly, the InP cap layer was etched by $H_3PO_4$and HCl with a ratio of 1:1. A Ti/Pt/Au p-metal contact was then deposited and patterned by a lift-off process to annular p+ Ohmic contact with 70-μm inside diameter. Subsequenetly, the p-InGaAs layer was etched by H_2SO_4:H_2O_2:H_2O (=1:1:10). A 92-μm-diamter PIN mesa was then formed by etching down into the n-InP contact layer. The n+ Ohmic contact was also realized by the same liftoff process of Ti/Pt/Au n-metal contact. Once the devices were isolated, the samples were covered with polyimide and annealed for passivation. Ti/Au interconnecting metal was then deposited to form the coplanar electrodes on top of the polyimide layer. Finally, the InP substrate was removed by using a combination of mechanical grinding and H_3PO_4: HCl (=3:1) chemical wet etching. Top-view optical micrograph of the fabricated InGaAs/InP absorption structure is shown in Fig. 2. After fabrication of the PIN absorption structure and the GMR grating, thermal epoxy was employed to assemble them together in the region with no pattern.

Atomic force microscope (AFM), which is a nondestructive method, is firstly employed to characterize the GMR grating structure and Fig. 3 shows the measured results. The period and thickness of the grating are 870 and 250 nm, respectively, while the width is 240 nm. The ideally etching depth of our designed GMR grating is 220 nm. However, the real etching depth of grating layer is 250 nm, which means that the overetching was occurred in the ICP-RIE processing, and the sidewall of waveguide as shown in the result of AFM testing in Fig. 3 is tilted due to imperfect etching process. Figure 4 shows scanning electron microscope (SEM) image of the fabricated GMR structure.

To measure the spectrum responses of the GMR grating structure, an Anritsu Tunics SCL tunable laser with a single-mode fiber pigtail was used as the light source. The GMR grating was illuminated by an input beam through the collimating fiber with normal incidence. A polarization controller was used to set polarization state of the input beam to TE or TM. Figure 5 shows the calculated and experimental spectrum results for both

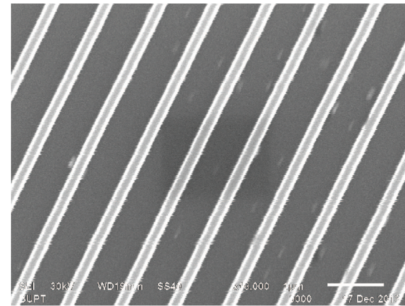

Fig. 4. (Color online) SEM images of the fabricated GMR grating.

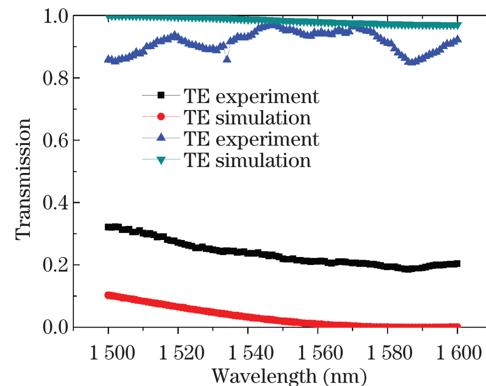

Fig. 5. (Color online) RCWA simulation and experimental spectral response of the fabricated GMR grating for TE and TM polarized light under normal incidence.

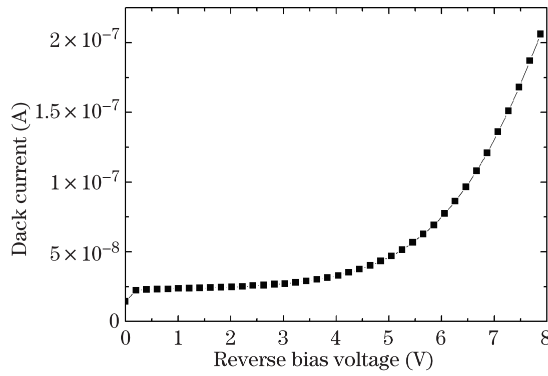

Fig. 6. Measured dark current as a function of reverse bias of the photodetector.

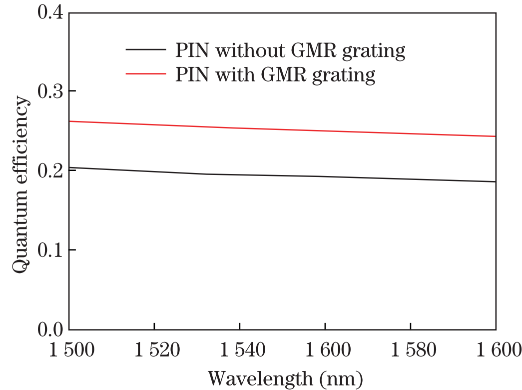

Fig. 7. (Color online) Response spectrum of the PIN photodetector with and without the GMR grating.

TE and TM polarizations. Transmission spectrum of the grating was calculated using RCWA simulation method and in this simulation, the relevant device parameters were extracted from the AFM images. We find that the transmission of the fabricated GMR grating is lower than 30% for TE-polarization, while the transmission for TM-polarization is more than 80% over a wavelength range of 100 nm (1500−1600 nm). Therefore, the reflection of the fabricated GMR grating is theoretically more than 70% for TE-polarization, since lossless absorption for silicon material at the wavelength band around 1550 nm.

The current−voltage characteristic of PIN photodetector without GMR grating was measured at room-temperature without illumination, as shown in Fig. 6. It indicates that the dark current of 27 nA was achieved at a reverse bias of −3.0 V, which can be attributed to several reasons such as imperfection of surface passivation[14], diffusion current, generation−recombination current, and tunneling current at high bias voltages[15].

Figure 7 shows optical response spectrum of the InGaAs/InP PIN absorption structure with and without the GMR grating under 3-V reverse bias. In this measurement, the input beam was collimated by a fiber collimator for TE-polarization at the wavelength range from 1500 to 1600 nm. Here, the InP/InGaAsPIN absorption structure with the GMR grating was fixed on the glass carrier of micro-manipulation stage. From the figure, one can see that quantum efficiencies of the PIN photodetectors with and without the GMR grating at the wavelength of 1550 nm are 25% and 19%, respectively, which indicates that the absorption of the i-InGaAs layer was enhanced by the reflection of the GMR grating, and consequently the quantum efficiency of the PIN structure.

In conclusion, a GMR grating is employed to improve the quantum efficiency of InGaAs/InP PIN photodetector for TE- polarization. The results show that the GMR grating can achieve high reflectivity for light at the wavelength range from 1500 to 1600 nm and the quantum efficiency increased by 31.6% for the InGaAs/InP PIN photodetector compared to no use of GMR. This GMR grating could be used for other photodetectors, such as unitraveling-carrier photodetctor (UTC-PD) and resonant-cavity enhanced photodetector (RCE-PD) in polarization sensitive systems.

This work was supported in part by the National Basic Research Program of China (No. 2010CB327600), the National Natural Science Foundation of China (Nos. 61020106007 and 61274044), the Natural Science Foundation of Beijing, China (No. 4132069), Program of Key International Science and Technology Cooperation Projects (No. 2011RR000100), the Fundamental Research Funds for the Central University (No. 2011RC 0403), 111 Project of China (No. B07005), Specialized Research Fund for the Doctoral Program of Higher Education of China (SRFDP) (No. 20130005130001), and the Program for Chang Jiang Scholars and Innovative Research Team in University, MOE (No. IRT0609).

References

1. R. J. Deri, E. C. M. Pennings, A. Scherer, A. S. Gozdz, C. Caneau, N. C. Andreadakis, V. Shah, L. Curtis, R. J. Hawkins, J. B. D. Soole, and J. I. Song, IEEE Photon. Technol. Lett. **4,** 1238 (1992).
2. V. Apalkov, G. Ariyawansa, A. G. U. Perera, M. Buchanan, Z. R. Wasilewski, and H. C. Liu, IEEE J. Quantum Electron. **46,** 877 (2010).
3. J. K. Yang, M. K. Seo, I. K. Hwang, S. B. Kim, and Y. H. Lee, Appl. Phys. Lett. **93,** 211103 (2008).
4. Y. Huang, C. Huang, Q. Wang, H. Huang, X. Wang, and X. Ren. Chin. Opt. Lett. **3,** 53 (2005).
5. K. Lai and J. C. Campbell, IEEE J. Quantum Electron. **30,** 108 (1994).
6. J. Yuan, B. Chen, and A. L. Holmes Jr, Electron Lett. **48,** 1230 (2012).
7. X. Duan, Y. Huang, X. Ren Y. Shang X. Fan, and F. Hu, IEEE Photon. Technol. Lett. **24,** 863 (2012).
8. K. J. Lee, J. Curzan, M. Shokooh-Saremi, and R. Magnusson, Appl. Phys. Lett. **98,** 211112 (2011).
9. Y. Ding and R. Magnusson, Opt. Express **12,** 5661 (2004).
10. X. Fan, Y. Huang, X. Ren, X. Duan, F. Hu, Q. Wang, S. Cai, and X. Zhang, Appl. Opt. **51,** 5767 (2012).
11. M. G. Moharam, D. A. Pommet, E. B. Grann, and T. K. Gaylord, J. Opt. Soc. Am. A. **12,** 1077 (1995).
12. M. G. Moharam, E. B. Grann, D. A. Pommet, and T. K. Gaylord, J. Opt. Soc. Am. A **12,** 1068 (1995).
13. I. C. Botten, M. S. Craig, R. C. McPhredran, J. L. Adams, and J. R. Andrewartha, Opt. Act. **28,** 413 (1981).
14. K. Kato, IEEE Trans. Microw. Theory Tech. **47,** 1265 (1999).
15. W. A. Wohlmuth, J.-W. Seo, P. Fay, C. Caneau, and I. Adesida, IEEE Photon. Technol. Lett. **91,** 388 (1997).